https://doi.org/10.5194/egusphere-2026-2386
Preprint. Discussion started: 20 May 2026

Lagged hydrological responses to glacier surface variability inferred from satellite-derived proxies in the Andes of central Chile

Ignacio Fuentes[a,b], Sebastian Morales[a,b], Nicolás Velasco[a], and Cristian Jordan[a]

[a]Facultad de Medicina Veterinaria y Agronomía, Universidad de Las Américas, Sede Providencia, Santiago, Chile
[b]Núcleo de Investigación en Sustentabilidad Agroambiental (NISUA), Universidad de las Américas, Santiago, Chile

Correspondence: Ignacio Fuentes (ifuentes@udla.cl)

Abstract. Glaciers sustain downstream water resources by providing delayed meltwater inputs, but ongoing climate change is rapidly altering their dynamics and associated hydrological responses. Understanding how glacier variability propagates through hydrological systems remains a key challenge, particularly in data-scarce mountain regions. This study characterises glacier surface dynamics and quantifies their lagged influence on streamflow, and explores associated vegetation responses, across glacierised catchments in central Chile. Multi-decadal Landsat observations were used to derive physically based glacier proxies, including snow-covered fraction, albedo, land surface temperature (LST), and snow elevation. Principal component analysis was applied to decompose glacier behaviour into dominant modes of long-term change, short-term variability, and temporal persistence, while prewhitened cross-correlation analysis was used to assess lagged relationships with downstream responses. Physical consistency among glacier proxies was evaluated to ensure coherent representation of glacier surface conditions. Results reveal a pervasive signal of glacier degradation, with most glaciers exhibiting declining trends in snow-covered fraction and albedo alongside increasing LST. Variability shows strong scale dependence, with contrasting glacier-level and regional trends driven by the influence of large glaciers, whereas temporal persistence exhibits a consistent increase across scales. Lagged analyses show a transition from glacier-dominated headwaters, where glacier variability precedes streamflow, to downstream basins where hydrological responses become increasingly decoupled from cryospheric processes. A regression framework linking glacier-response modes to hydrological lag explains a substantial fraction of variability in streamflow timing ($R^2 \sim 0.72$). Vegetation responses are spatially heterogeneous and not significant at the system scale. These findings demonstrate the potential of satellite-based approaches to quantify the timing, persistence, and propagation of cryospheric signals in data-scarce mountain regions.

1 Introduction

Mountain glaciers are among the most sensitive components of the Earth system to climatic variability and long-term warming (Owen et al., 2009; Winkler et al., 2010). Changes in temperature, precipitation, and surface energy balance rapidly translate into shifts in glacier mass balance, snow cover, and meltwater production (Oerlemans, 2005; Zemp et al., 2015). Over recent decades, widespread glacier retreat has been documented across most mountain regions of the world, including the Andes of South America (Rabatel et al., 2013; Zemp et al., 2019). These changes not only alter glacier geometry and mass balance but

https://doi.org/10.5194/egusphere-2026-2386
Preprint. Discussion started: 20 May 2026

also have important implications for downstream hydrology, particularly in regions where meltwater contributes significantly to seasonal water availability (Nie et al., 2021; Pradhananga and Pomeroy, 2022).

Glaciers and seasonal snowpack act as natural reservoirs that regulate streamflow by storing water during cold periods and releasing it during warmer months (Jansson et al., 2003; Stewart, 2009). This buffering capacity is especially important in regions characterised by strong seasonality in precipitation, where meltwater sustains river discharge during dry periods (Ohlanders et al., 2013; Bravo et al., 2017). However, ongoing glacier retreat and declining snow accumulation are expected to modify both the magnitude and timing of meltwater contributions, potentially altering hydrological regimes and increasing water stress in glacier-fed basins (Hanzer et al., 2018; Garreaud et al., 2020).

Satellite remote sensing has become an essential tool for monitoring glacier dynamics at regional and multi-decadal scales, overcoming the spatial and logistical limitations of field observations (Bamber and Rivera, 2007; Rabatel et al., 2017). Long-term multispectral archives such as Landsat provide consistent observations that enable the retrieval of key glacier surface properties, including snow-covered area, surface albedo, land surface temperature (LST), and snowline elevation (Raup et al., 2007; Racoviteanu et al., 2021). Together, these variables provide valuable information about glacier surface energy balance and seasonal melt processes (Menenti et al., 2020; Gunnarsson et al., 2023).

Among these indicators, the fraction of glacier area classified as snow is particularly informative in heterogeneous mountain environments because it provides a normalised measure of glacier snow persistence that is comparable across glaciers of different size (Salomonson and Appel, 2006; Racoviteanu et al., 2009). Additionally, it may be considered a proxy for the accumulation area ratio (AAR) when evaluated near the end of the ablation season, although it represents a snow-cover metric rather than a direct estimate of mass balance (Rabatel et al., 2017; Rastner et al., 2019). Surface albedo plays a central role in glacier energy balance by controlling the absorption of incoming solar radiation, while LST provides an indirect indicator of melt conditions and surface energy exchange (Greuell and Knap, 2000; Wu et al., 2015). Elevation-based metrics such as snow elevation further provide insights into glacier mass-balance regimes and their response to climatic forcing (Rabatel et al., 2017).

Despite these advances, the extent to which satellite-observed glacier surface signals translate into downstream hydrological responses, and the characteristic timescales of these responses, remains limited. While numerous studies have documented glacier change and meltwater contributions (Gascoin et al., 2011; Ohlanders et al., 2013; Bravo et al., 2017; Ayala et al., 2020), fewer have explicitly quantified the temporal relationships between glacier surface signals and streamflow, particularly in terms of lagged responses (Radić and Hock, 2014; Huss et al., 2017). Time series of glacier surface variables and streamflow often exhibit strong seasonality and autocorrelation, which can obscure physically meaningful relationships if not properly accounted for (Zwiers and Von Storch, 2004). Statistical approaches such as prewhitened cross-correlation analysis provide a robust framework for identifying characteristic response times between variables by removing shared temporal structure and serial dependence (Box et al., 2015*a*).

In addition to cryospheric controls, vegetation dynamics may influence hydrological variability through their effects on evapotranspiration and soil moisture storage (Jiao et al., 2017; Liu et al., 2018). Satellite-derived vegetation indices, such as the Normalised Difference Vegetation Index (NDVI), provide a means to investigate potential ecohydrological interactions along-

https://doi.org/10.5194/egusphere-2026-2386
Preprint. Discussion started: 20 May 2026

side glacier-driven processes within a lag-aware analytical framework (Pettorelli et al., 2005). Analysing these components within a unified framework offers an opportunity to disentangle the relative timing and influence of glacier and vegetation signals on streamflow. However, in this study vegetation is treated as a secondary response variable, allowing us to evaluate whether glacier-driven signals propagate beyond hydrological processes into ecosystem dynamics.

The objectives of this study are therefore to: (1) quantify multi-decadal trends in glacier surface properties using satellite-derived indicators, including the fraction of glacier area covered by snow, surface albedo, LST, and snow elevation metrics; (2) evaluate the robustness and physical consistency of these glacier surface proxies, and characterise their dominant modes of variability using principal component analysis; (3) identify lagged relationships between glacier surface conditions and downstream streamflow using prewhitened cross-correlation analysis; and (4) explore the relative timing of hydrological and vegetation responses to glacier variability across catchments. Vegetation analyses are included as a complementary component to explore whether glacier variability influences the timing of ecosystem responses, in addition to hydrological processes. To demonstrate the applicability of this framework, we apply it to glacierised basins in central Chile, where snowpack and glacier melt play a critical role in sustaining water supply for urban consumption, agriculture, and ecosystems under a Mediterranean climate (Beck et al., 2018; Ohlanders et al., 2013; Bravo et al., 2017). Additionally, this region has experienced sustained glacier mass loss since the mid-20th century, primarily driven by regional warming and reduced winter snow accumulation (Le Quesne et al., 2009; Masiokas et al., 2016; Ayala et al., 2020), and prolonged drought conditions, which have affected ecosystems (Miranda et al., 2023; Fuentes et al., 2025) and increased reliance on cryospheric resources (Masiokas et al., 2016; Garreaud et al., 2017; Ayala et al., 2020).

2 Materials and methods

2.1 Study area

The study area comprises glacierised Andean catchments located in the Valparaíso and Metropolitana regions of central Chile (Figure 1). These basins extend from low-elevation foothills (500-1000 m a.s.l.) to high-mountain environments exceeding 4000 m a.s.l., and drain westward toward the Pacific Ocean. Glacierised areas are primarily concentrated in the headwaters of major river systems, including tributaries of the Maipo and Aconcagua basins.

The Metropolitana Region is the most populated region of Chile, while Valparaíso ranks third (Aprigliano et al., 2024). Together, they account for 50.8% of the country's total population. Water supply for urban consumption, agriculture, and ecosystems in these regions depends strongly on Andean water resources, particularly seasonal snowpack and, to a lesser extent, glacier melt (Webb et al., 2021). Consequently, changes in cryospheric conditions have direct implications for regional water availability and drought resilience (Gascoin et al., 2011; Ayala et al., 2020).

The regional climate is Mediterranean to semi-arid, characterised by cool, wet winters and warm, dry summers (Beck et al., 2018). Snow accumulation during winter and melt during spring and summer dominate the seasonal hydrological cycle, producing a mixed runoff regime in which winter discharge is largely rainfall-driven, while spring and summer runoff is sustained by delayed snow and glacier melt contributions (Rodriguez et al., 2014; Mernild et al., 2017). This seasonal decoupling between

https://doi.org/10.5194/egusphere-2026-2386
Preprint. Discussion started: 20 May 2026

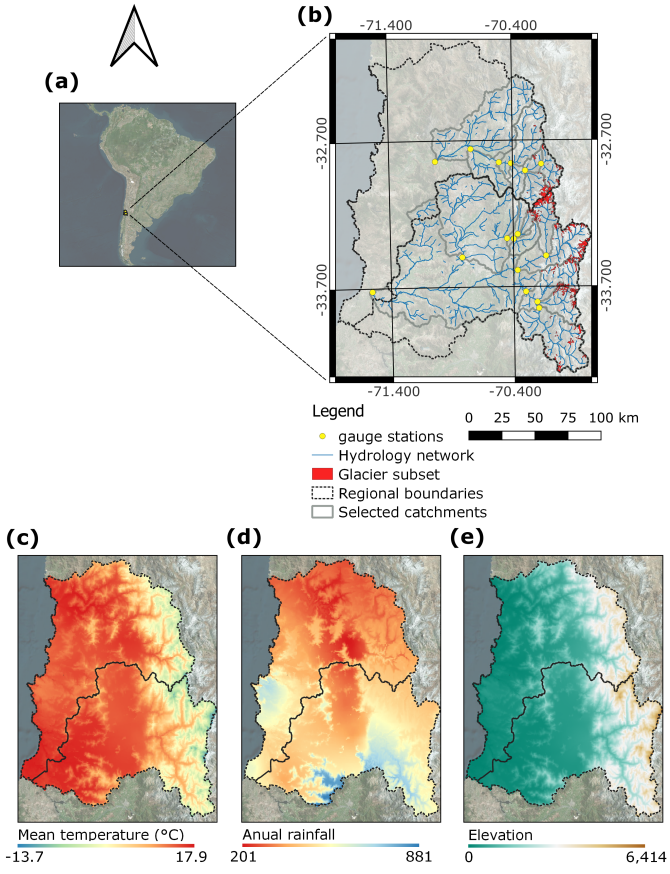

Figure 1. Study area in central Chile. (a) Location of the study region within South America. (b) Glacierised catchments in the Valparaíso and Metropolitana regions, including river networks and gauging stations used for hydrological analysis. (c-e) Spatial distribution of mean annual temperature, annual precipitation (WorldClim v1; Hijmans et al., 2005), and elevation (NASA DEM; Jpl, 2020), illustrating the strong climatic and topographic gradients across the study area. Glacierised areas are concentrated in high-elevation headwaters of the Maipo and Aconcagua river basins.

precipitation and runoff introduces characteristic temporal lags in hydrological response. Interannual variability is high, and the region has experienced persistent drought conditions over recent decades, particularly during the Central Chilean megadrought (Garreaud et al., 2020).

These pronounced climatic and topographic gradients make the study region particularly suitable for investigating spatial variability in glacier-hydrology interactions and associated response times.

https://doi.org/10.5194/egusphere-2026-2386
Preprint. Discussion started: 20 May 2026

2.2 Datasets

2.2.1 Glacier inventory

Glacier outlines and attributes were obtained from the Chilean public glacier inventory (updated 2022; https://dga.mop.gob.cl/inventario-publico-de-glaciares-actualizacion-2022/), produced by the Dirección General de Aguas (DGA). The inventory includes glacier type classification, geographic location, and polygon geometries derived from semi-automated delineation of Landsat imagery.

The glacier inventory was filtered to retain valley and mountain glaciers within the Valparaíso and Metropolitana regions, excluding other types (e.g., rock glaciers) to focus on ice bodies with well-defined seasonal snow signals suitable for optical remote sensing. This resulted in a total of 174 glaciers.

2.2.2 Satellite imagery and topography

Multi-temporal optical and thermal imagery was derived from the Landsat archive, including Landsat 5 TM, Landsat 7 ETM+, and Landsat 8–9 OLI/TIRS sensors, covering the period from the mid-1980s to 2025 (Markham and Helder, 2012; Irons et al., 2012; Roy et al., 2014; Masek et al., 2020). Analysis was based on surface reflectance products, providing atmospherically corrected multispectral data at 30 m spatial resolution, with a nominal revisit time of 16 days per satellite.

Spectral bands were used to derive indices, broadband surface albedo, and LST. To support terrain-based analyses, topographic data were obtained from the NASA Digital Elevation Model (NASA DEM), a reprocessed version of Shuttle Radar Topography Mission (SRTM) data. The DEM was used for elevation statistics, topographic shadow detection, and illumination correction (Crippen et al., 2016).

2.2.3 Hydrologic data and catchment boundaries

Daily streamflow records were obtained from the Explorador Climático platform of the Center for Climate and Resilience Research (CR2; https://explorador.cr2.cl/), which hosts quality-controlled data from the national hydrometric network managed by the DGA. Gauging stations were selected based on data availability and spatial correspondence with glacierised catchments. Only stations with at least 240 overlapping monthly observations (equivalent to 20 years of data) after aggregation, deseasonalisation, and alignment with glacier-derived time series were retained for analysis.

Catchment boundaries were obtained from the Catchment Attributes and MEteorology for Large Sample Studies dataset for Chile (CAMELS-CL; https://camels.cr2.cl/), which provides standardised basin delineations upstream of hydrometric stations. These geometries enable consistent linkage between glacier properties, streamflow records, and downstream analyses (Alvarez-Garreton et al., 2018).

https://doi.org/10.5194/egusphere-2026-2386
Preprint. Discussion started: 20 May 2026

2.2.4 Vegetation data

Vegetation activity was characterised using the PKU (Peking University) Normalised Difference Vegetation Index (NDVI) dataset from the Global Inventory Modeling and Mapping Studies (GIMMS), accessed via Google Earth Engine (https://gee-community-catalog.org/projects/gimms_ndvi/). This dataset provides a temporally consistent long-term NDVI record (1982–2022), based primarily on Advanced Very High Resolution Radiometer (AVHRR) observations and extended through cross-sensor calibration and continuity corrections, enabling robust multi-decadal vegetation analyses (Li et al., 2023).

2.3 Preprocessing of satellite data

Satellite imagery was processed in Google Earth Engine (Gorelick et al., 2017) using a consistent workflow across Landsat sensors (L5, L7, L8, and L9) (Figure 2). Surface reflectance products were harmonised and scaled to physical units. Clouds and shadows were masked using quality assurance bands and thermal filtering, while terrain-induced effects were reduced using a hybrid topographic correction involving the application of Minnaert and C-corrections (Smith et al., 1980; Teillet et al., 1982).

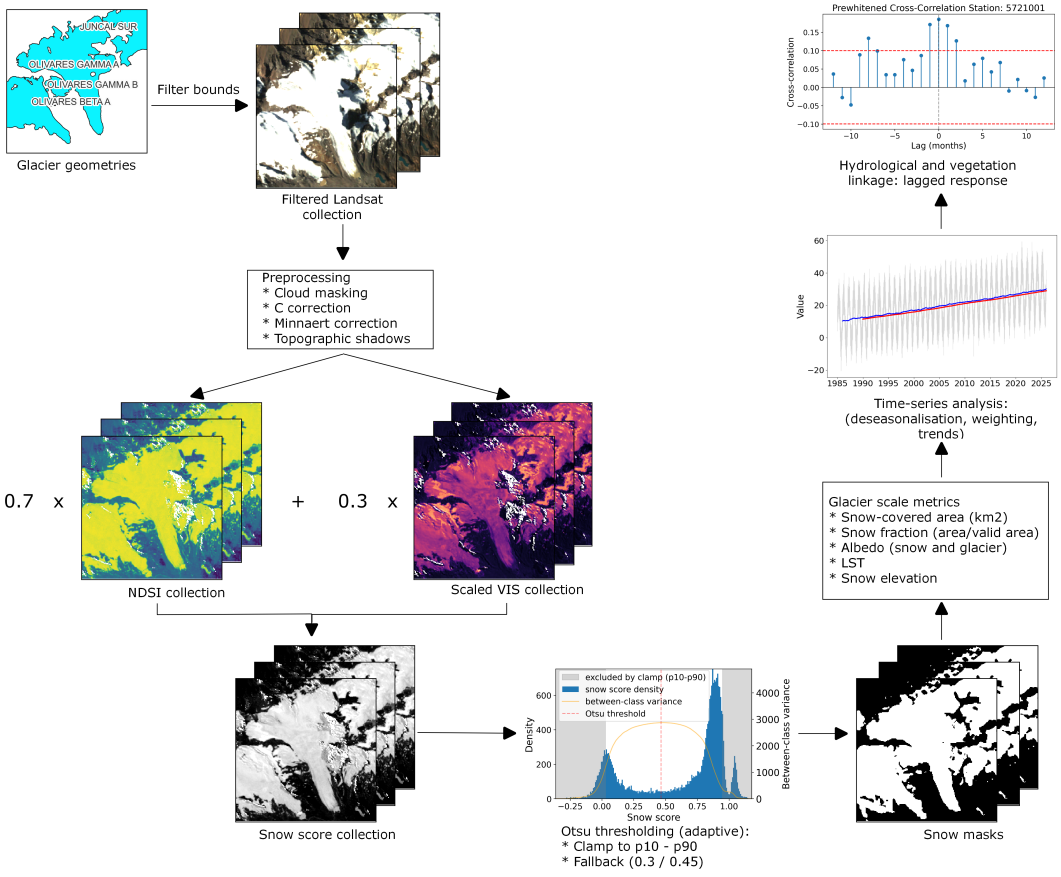

Figure 2. Workflow for regional glacier snow signal detection and hydro-climatic linkage analysis.

https://doi.org/10.5194/egusphere-2026-2386
Preprint. Discussion started: 20 May 2026

Scenes with insufficient valid glacier coverage (<70%) were excluded to ensure robust temporal sampling. After preprocessing, 1982 scenes spanning 1984–2026 were retained (Table 1). For each glacier and date, spatial statistics were computed to summarise surface conditions and reduce sensitivity to residual noise.

Table 1. Summary of Landsat imagery used in this study, including sensor, acquisition period, WRS-2 path–row combinations, and number of usable scenes after preprocessing.

Satellite	Date range	WRS-2 Path–Row	Scenes
Landsat 5	14-10-1984 to 17-11-2011	232/083	196
		233/083	173
		233/084	189
Landsat 7	12-07-1999 to 07-01-2024	232/083	270
		233/083	280
		233/084	272
Landsat 8	02-04-2013 to 25-12-2025	232/083	140
		233/083	153
		233/084	159
Landsat 9	06-12-2021 to 26-12-2025	232/083	48
		233/083	50
		233/084	52
Total			**1982**

2.4 Snow quantification and glacier proxies

Snow-covered areas within glacier outlines were identified using an adaptive, physically based classification approach that combines spectral indices, surface brightness, and illumination information. Snow detection relied on topographically corrected Landsat surface reflectance data and was designed to remain robust across sensors, seasons, and varying snow conditions.

2.4.1 Spectral indices

The Normalised Difference Snow Index (NDSI) was computed as:

$$NDSI = \frac{\rho_{green} - \rho_{SWIR1}}{\rho_{green} + \rho_{SWIR1}} \quad (1)$$

where ρ_{green} and ρ_{SWIR1} correspond to topographically corrected surface reflectance in the green and shortwave infrared (SWIR) bands, respectively. NDSI exploits the high reflectance of snow in the visible spectrum and its strong absorption in the SWIR, and is widely used for snow and ice detection in mountain environments (Salomonson and Appel, 2004).

https://doi.org/10.5194/egusphere-2026-2386
Preprint. Discussion started: 20 May 2026

To complement NDSI, a visible-band brightness metric (VIS) was also computed as the mean of blue, green, and red reflectance bands and rescaled to the 0–1 range. This term provides information on overall surface brightness and helps distinguish snow from darker debris-covered ice or rock surfaces.

2.4.2 Composite snow likelihood metric

Snow detection was based on a composite metric defined as:

$$snowScore = 0.7 \times NDSI + 0.3 \times VIS \tag{2}$$

Both components were normalised prior to combination. The weighting was chosen to prioritise the physical sensitivity of NDSI to snow presence (dominant weight of 0.7), while retaining a secondary contribution from surface brightness (weight of 0.3) to stabilise classification in cases where NDSI alone becomes ambiguous.

2.4.3 Adaptive thresholding using Otsu's method

Snow classification was performed using adaptive thresholds derived from Otsu's method, which identifies the threshold that maximises inter-class variance in the snowScore histogram (Yin et al., 2013):

$$\sigma_B^2(t) = \omega_1(t)\,\omega_2(t)\,[\mu_1(t) - \mu_2(t)]^2 \tag{3}$$

where ω_1 and ω_2 represent the proportions of pixels assigned to each class separated by threshold t, and μ_1 and μ_2 are the corresponding class means. The optimal threshold t^* maximises $\sigma_B^2(t)$.

To ensure stability across varying conditions, thresholds were constrained within percentile-based bounds (10th–90th percentiles). In cases of poorly separable (unimodal) distributions, fallback thresholds (0.3 or 0.45) were applied when one class dominated more than 90% of pixels. This approach ensures robust snow detection across seasonal and interannual variability.

2.4.4 Topographic shadows

Topographic shadows were identified in Landsat scenes using solar geometry and DEM-based illumination modelling (NASADEM; Jpl, 2020). Shadow information was used to assess observation quality but was not used to exclude pixels from snow classification. For albedo estimation, only illuminated pixels were considered.

2.4.5 Glacier-scale proxies

For each glacier and acquisition date, glacier-scale proxies were derived from the classified snow mask and associated fields:

Snow-covered fraction: Snow-covered area was computed as the area of pixels classified as snow within the glacier outline and normalised by the area of valid (observed) pixels. This normalisation accounts for data gaps due to clouds, shadows, and

https://doi.org/10.5194/egusphere-2026-2386
Preprint. Discussion started: 20 May 2026

sensor artefacts, yielding an observation-corrected snow-covered fraction. When evaluated during the late ablation season, this metric may approximate the accumulation area ratio (AAR), although it is not strictly equivalent (Salomonson and Appel, 2004; Aberle et al., 2025).

Surface albedo: Broadband shortwave albedo was estimated from topographically corrected Landsat reflectance using a linear narrowband-to-broadband conversion based on visible, near-infrared, and shortwave infrared bands (Liang, 2001; Traversa et al., 2021). Albedo was summarised as the median over (i) all glacier pixels and (ii) snow-covered, illuminated pixels.

Land surface temperature: Land surface temperature (LST) was derived from Landsat thermal bands (Sobrino et al., 2004) and summarised as the median over glacier pixels.

Snow-covered elevation metrics: The elevation distribution of snow-covered pixels was characterised using median and mean elevations derived from the NASA DEM, providing a measure of the vertical structure of snow cover (Racoviteanu et al., 2008).

2.5 Physical consistency assessment

The physical consistency of glacier-scale proxies was evaluated using a cross-variable diagnostic framework at the individual-glacier level. This approach assesses whether independently derived proxies exhibit coherent behaviour consistent with established cryospheric relationships (Hock, 2005; Rabatel et al., 2013), providing a process-based internal validation of proxy reliability without relying on external observations.

Proxy time series were aggregated to monthly resolution for each glacier using median statistics. To reduce the influence of poorly constrained observations, monthly values were retained only when (i) the valid observed glacier area exceeded 5 hectares and (ii) snow-covered fraction ranged between 0.05 and 0.95, excluding near-complete snow absence or full snow cover.

Deseasonalisation was performed independently for each glacier and proxy by removing the glacier-specific mean seasonal cycle. Spearman rank correlations were then computed between deseasonalised snow-covered fraction and other proxies (LST, albedo, and snow-covered elevation), requiring a minimum of 24 valid observations. Expected physical relationships include negative correlations with LST, positive correlations with albedo, and negative relationships with elevation-based metrics reflecting upward snowline migration under reduced snow conditions.

The proportion of glaciers exhibiting correlations with signs opposite to physical expectations was quantified for each proxy pair. Elevated fractions of unexpected relationships were interpreted as indicative of local complexity, observational limitations, or proxy ambiguity. Together, these diagnostics provide a quantitative assessment of the physical coherence and interpretability of glacier-scale proxies.

In addition to correlation-based diagnostics, the robustness of regional trend estimates was assessed using a year-block bootstrap approach. Monthly deseasonalised regional time series were resampled by complete calendar years with replacement to preserve temporal dependence. For each bootstrap realisation, linear trends were re-estimated, and median slopes and 95% confidence intervals were derived from the resulting distributions (Politis and Romano, 1994).

https://doi.org/10.5194/egusphere-2026-2386
Preprint. Discussion started: 20 May 2026

2.6 Deseasonalisation and trend analysis

All glacier-scale proxy time series were aggregated to monthly resolution using median values. Deseasonalisation was performed using harmonic regression (two annual harmonics), removing the dominant seasonal cycle while preserving interannual variability (Box et al., 2015*b*). From these deseasonalised series, linear trends were estimated using ordinary least squares regression, with time expressed in fractional years.

Trend analysis was conducted at both regional and glacier scales. Regional time series were computed using water-equivalent-weighted aggregation to account for glacier size, while glacier-level trends were estimated individually and summarised to characterise spatial heterogeneity. Additionally, short-term variability and temporal persistence were quantified using rolling standard deviation (SD) and lag-1 autocorrelation (AC1), computed over an 84-month window to ensure stable estimation of variability and autocorrelation while retaining sensitivity to interannual and decadal variability. Trends in these metrics were also analysed at both regional and glacier scales.

2.7 Lagged analysis with streamflow and vegetation

Lagged relationships between glacier variability and downstream responses were quantified using prewhitened cross-correlation functions (CCF) across multiple hydrometric stations. For each gauged catchment, glaciers from the national inventory within the corresponding CAMELS-CL basin polygons were selected by spatial overlay. Glacier-scale proxy time series were aggregated to catchment scale using a water-equivalent-weighted mean, and subsequently aggregated to monthly resolution and deseasonalised (Section 2.6) prior to analysis, yielding an effective glacier signal that emphasises the contribution of larger ice bodies.

2.7.1 Prewhitening

To account for serial dependence, prewhitening was applied prior to cross-correlation analysis. For each station and glacier proxy, an autoregressive model AR(p) was fitted using automatic order selection (`auto_arima`, with $0 \leq p \leq 3$ and $q = 0$; Shumway and Stoffer, 2017). The resulting filter was applied to both the glacier proxies (x_t) and the corresponding response series (y_t; discharge or NDVI):

$$x'_t = x_t - \sum_{k=1}^{p} \phi_k x_{t-k} \tag{4}$$

$$y'_t = y_t - \sum_{k=1}^{p} \phi_k y_{t-k} \tag{5}$$

where ϕ_k are the autoregressive coefficients at lag k. This ensures comparable autocorrelation structure between series and reduces spurious correlations arising from shared autocorrelation and persistence.

https://doi.org/10.5194/egusphere-2026-2386
Preprint. Discussion started: 20 May 2026

2.7.2 Cross-correlation and spatial diagnostics

Prewhitened cross-correlations were computed for lags within ± 12 months (Box et al., 2015*b*; Shumway and Stoffer, 2017). For each station, the lag corresponding to the maximum absolute correlation was retained as summary metrics and mapped across the basin network. Statistical significance was assessed using an approximate confidence bound of $\pm 2/\sqrt{n}$, where n is the number of overlapping observations. Lag interpretations were restricted to plausible hydrological and ecohydrological response times and were not interpreted as evidence of causality.

2.8 Decomposition of glacier-response modes

To characterise dominant patterns of glacier behaviour, glacier-scale proxy time series were summarised using three classes of metrics derived from deseasonalised monthly series: (i) long-term trends, (ii) short-term variability, and (iii) temporal persistence. Trend metrics correspond to linear slopes estimated using ordinary least squares. Variability was quantified as the standard deviation of deseasonalised monthly anomalies, while memory was computed as the lag-1 autocorrelation, representing temporal persistence (Box et al., 2015*b*).

Separate principal component analyses (PCA) were applied to each group of metrics across glaciers to extract dominant co-variability patterns. Variables were standardised to zero mean and unit variance prior to analysis, and the first principal component (PC1) was retained as a summary index representing the dominant trend, variability, and memory modes (Jolliffe and Cadima, 2016). To investigate structural controls, PCA scores were correlated with glacier inventory properties, including area, volume, slope, elevation, and latitude, using Pearson correlation coefficients.

2.9 Linking glacier-response modes to hydrological lag

To assess whether glacier-response modes relate to downstream hydrological timing, we fitted a multiple linear regression model relating catchment-scale PCA scores to the lag of maximum significant cross-correlation between glacier proxies and streamflow. Predictors correspond to the first principal component (PC1) scores of the trend, variability, and memory modes aggregated at the catchment scale, while the response variable is the lag (in months) associated with the maximum statistically significant cross-correlation.

All variables were standardised prior to model fitting to allow direct comparison of regression coefficients. Model performance was evaluated using the coefficient of determination (R^2), and statistical significance was assessed using standard t-tests on regression coefficients. To account for potential dependencies arising from nested catchments, a sensitivity analysis was performed using cluster-robust standard errors at the basin level (Colin Cameron and Miller, 2015).

https://doi.org/10.5194/egusphere-2026-2386
Preprint. Discussion started: 20 May 2026

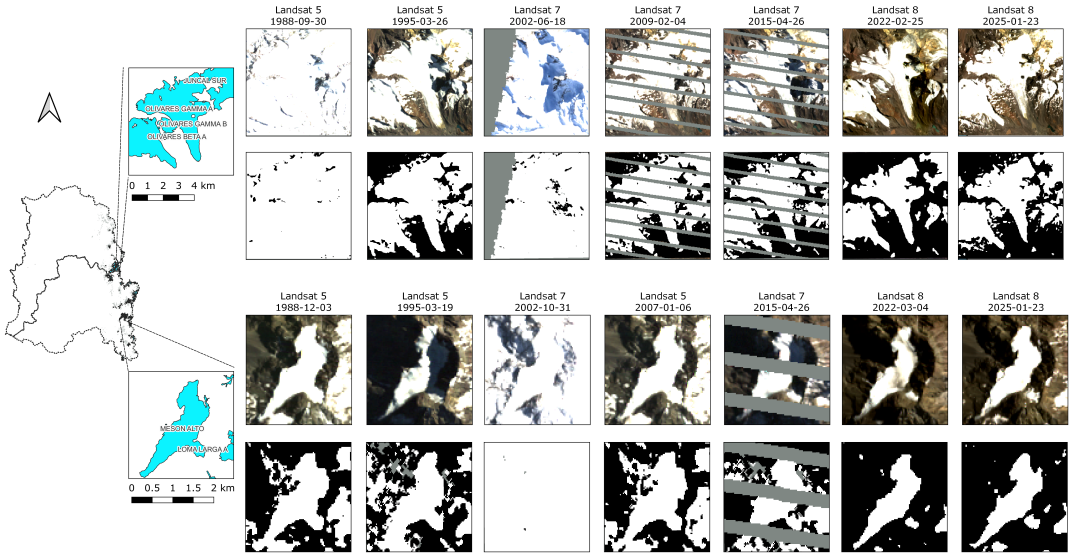

Figure 3. Examples of snow classification across two representative glaciers using multi-temporal Landsat imagery. For each glacier, RGB composites (top rows) are shown alongside the corresponding binary snow masks (bottom rows) derived from the adaptive SnowScore thresholding approach. Scenes span multiple sensors (Landsat 5, 7, and 8) and a range of acquisition dates and snow conditions. Classification is depicted as white, black, and grey for snow, no-snow, and masked pixels, respectively.

3 Results

3.1 Qualitative evaluation and behaviour of adaptive snow classification

The performance of the snow classification approach was first assessed through visual inspection of multi-temporal Landsat imagery and corresponding snow masks (Figure 3). Across sensors and acquisition dates, the method consistently delineates snow-covered areas while preserving spatial coherence with glacier geometry and topography. Snow masks capture both extensive winter snow cover and more fragmented conditions during transitional periods, and remain robust under varying illumination, shadowing, and sensor-specific artefacts (e.g., Landsat 7 SLC-off gaps). These examples provide qualitative evidence that the classification captures physically realistic patterns of snow distribution. These patterns are consistent across the full Landsat archive and are not sensitive to sensor transitions or data gaps.

Beyond visual consistency, the adaptive thresholds remain stable through time, typically ranging between 0.30 and 0.45 without evidence of systematic drift (Figure S1, Supplementary materials). This stability indicates robustness to varying acquisition conditions and sensor transitions. Threshold values increase with snow-covered fraction, reflecting stricter classification under snow-rich conditions and more permissive detection when snow is sparse. This coherent, non-linear relationship confirms that threshold selection responds to surface conditions rather than varying randomly.

https://doi.org/10.5194/egusphere-2026-2386
Preprint. Discussion started: 20 May 2026

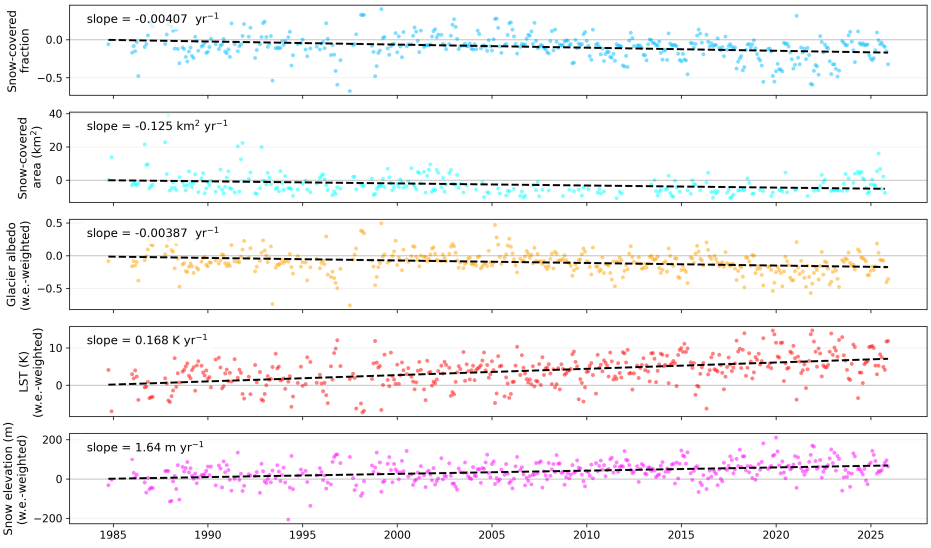

Figure 4. Long-term evolution and trends (dhashed lines) of regional glacier-scale proxies (1984–2025) derived from Landsat observations. Time series represent deseasonalised monthly anomalies aggregated at the regional scale.

3.2 Temporal variability of glacier-scale proxies

Glacier-scale proxies derived from satellite observations exhibit consistent seasonal and interannual variability across all analysed glaciers (Figure S2, Supplementary materials). Snow-covered fraction shows a strong seasonal cycle, with near-complete snow cover during winter and reduced values during summer, although the amplitude and persistence of snow cover vary across glaciers. Surface albedo follows a similar seasonal pattern, with higher values during snow-covered periods and lower values when exposed ice or debris dominates.

LST displays a clear inverse seasonal behaviour, with higher temperatures during summer and lower values during winter, consistent with expected energy balance dynamics. Elevation-based snow proxies exhibit comparatively lower variability but reflect gradual shifts associated with changes in snow distribution and melt processes.

Despite differences among glaciers, the coherence of seasonal patterns across variables indicates that the derived proxies capture physically consistent glacier dynamics. These time series provide the basis for subsequent analyses of long-term trends and hydro-climatic linkages.

3.3 Long-term trends in glacier-scale proxies

Regional glacier-scale proxies exhibit consistent long-term changes over the study period (Figure 4). Snow-covered fraction shows a significant negative trend ($p < 0.001$), indicating a progressive reduction in snow cover. This decline is accompanied by decreasing glacier albedo and increasing LST, reflecting reduced surface reflectivity and enhanced surface warming.

https://doi.org/10.5194/egusphere-2026-2386
Preprint. Discussion started: 20 May 2026

Elevation-based metrics exhibit positive trends, indicating an upward migration of the snowline, while total snow-covered area also declines when restricting the analysis to high-quality observations ($\geq 99\%$ valid glacier area), although its magnitude is sensitive to data completeness. This contrasts with the more robust behaviour of normalised metrics such as snow-covered fraction. Together, these changes point to reduced snow persistence and enhanced melt conditions.

At the individual glacier scale, trends show substantial spatial variability and are less frequently statistically significant (Figure 5). Despite this, glacier-level slopes exhibit clear directional consistency across the region. Most glaciers show decreasing snow-covered fraction and albedo, alongside increasing LST and snow elevation. Specifically, 97% of glaciers exhibit negative trends in snow-covered fraction and albedo, while 98.8% and 76.3% show positive trends in LST and median snow elevation, respectively.

3.4 Trends in variability and temporal persistence

Beyond changes in mean glacier conditions, we evaluated temporal dynamics using rolling standard deviation (SD) and lag-1 autocorrelation (AC1) of deseasonalised monthly time series. At the regional scale, weighted aggregation reveals a general decrease in variability for snow-covered fraction, albedo, and snow elevation, accompanied by a consistent increase in temporal persistence (Figure S3, Supplementary materials). In contrast, glacier-level variability trends show substantial heterogeneity, with many glaciers exhibiting weak or opposite changes (Figure S4). This apparent discrepancy reflects the influence of glacier size in the regional aggregation. Weighted regional SD trends often diverge from the distribution of glacier level trends. For instance, snow-covered fraction exhibits a positive median trend in variability across glaciers, but a negative weighted regional trend (Table S1, Supplementary materials). This scale dependence is supported by a significant negative relationship between glacier size and variability trends (Spearman $\rho = -0.47$, $p < 10^{-9}$ for snow-covered fraction), indicating that larger glaciers tend to exhibit decreasing variability over time, while smaller glaciers more frequently show increasing variability. Similar relationships are observed for albedo ($\rho = -0.29$), LST ($\rho = -0.35$), and snow elevation ($\rho = -0.21$).

In contrast, trends in temporal persistence (AC1) are largely consistent across scales. Both regional and glacier-level analyses show widespread increases in lag-1 autocorrelation, with positive median and weighted-median slopes across all proxies, except for LST at the regional scale. This indicates a coherent system-wide increase in temporal persistence that is largely independent of glacier size or aggregation approach. Together, these results indicate that variability and persistence capture distinct aspects of glacier dynamics, where variability reflects heterogeneous and scale-dependent responses, whereas persistence exhibits a robust, spatially coherent signal across the glacier system.

3.5 Physical consistency assessment

To evaluate whether the observed trends reflect robust and physically meaningful glacier responses, we first assess the stability of regional trends using a year-block bootstrap approach (Figure 6A). All glacier proxies exhibit consistent trend estimates with narrow confidence intervals that do not overlap zero, indicating that the observed long-term changes are statistically robust and not driven by temporal sampling variability.

https://doi.org/10.5194/egusphere-2026-2386
Preprint. Discussion started: 20 May 2026

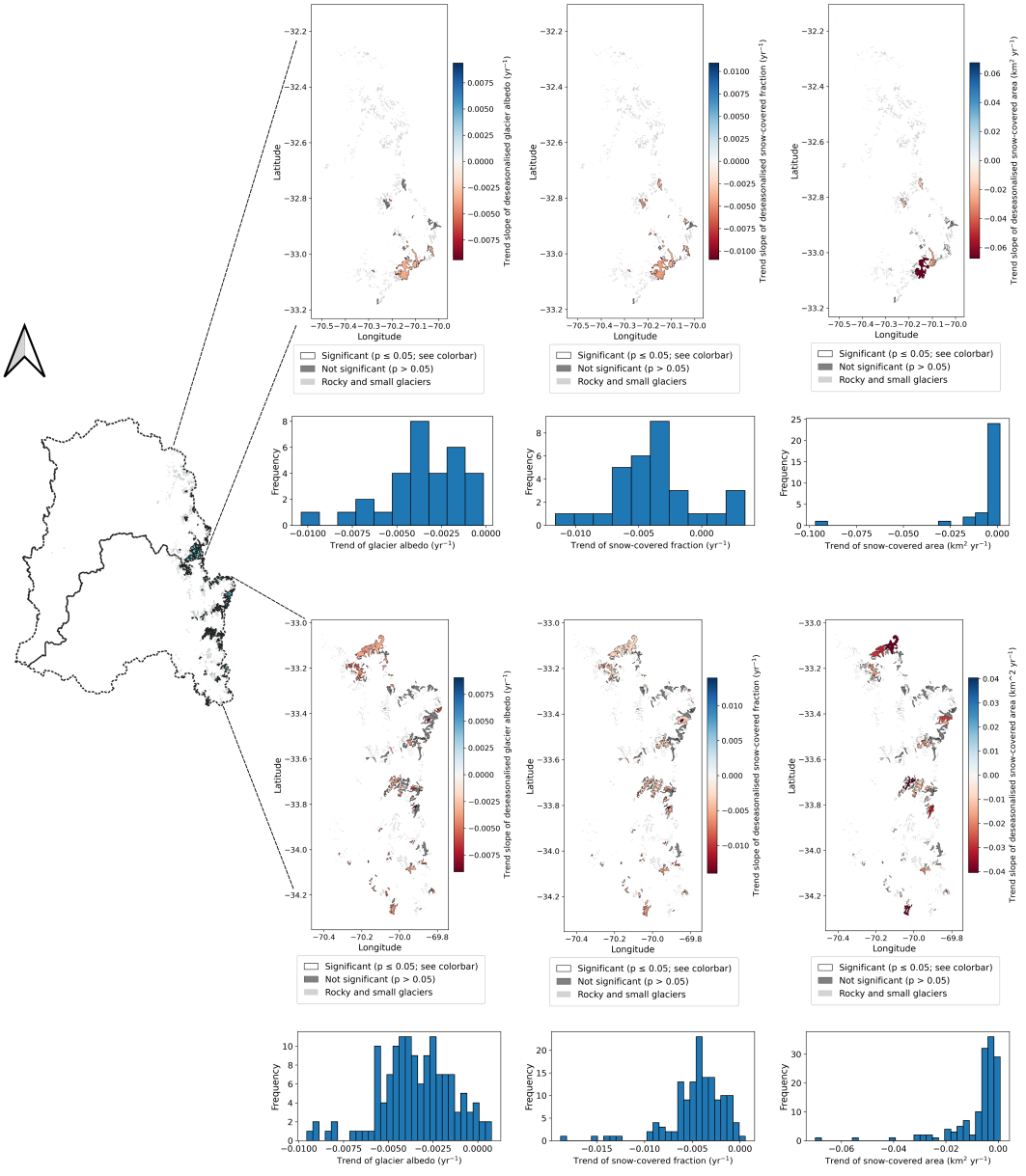

Figure 5. Spatial distribution and frequency histograms of glacier-specific long-term trends in glacier albedo, snow-covered fraction, and snow-covered area across the study region. Colored glaciers indicate statistically significant trends ($p \leq 0.05$), while grey glaciers denote non-significant trends. Histograms illustrate the distribution of glacier-level slopes, highlighting consistent directional behaviour despite spatial variability.

https://doi.org/10.5194/egusphere-2026-2386
Preprint. Discussion started: 20 May 2026

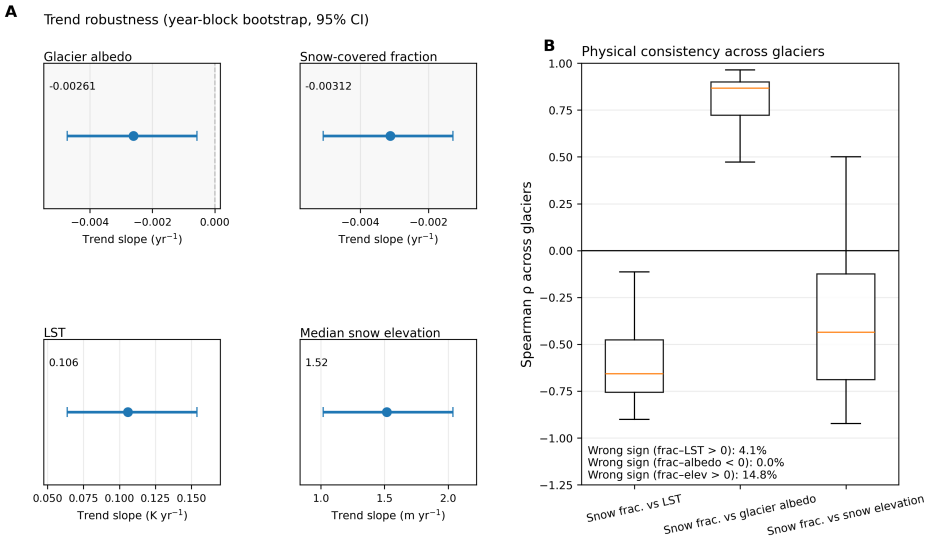

Figure 6. Robustness and physical consistency of glacier-scale proxies displaying: (A) Trend robustness assessed using year-block bootstrap confidence intervals for monthly deseasonalised regional anomalies. Points indicate median slope estimates and horizontal bars show 95% confidence intervals; and (B) Physical consistency across glaciers assessed from Spearman correlations computed at the individual glacier level using monthly deseasonalised time series. Boxplots summarise the distribution of glacier-level correlations.

The analysis of the consistency of relationships among glacier-scale proxies across individual glaciers after deseasonalisation is in Figure 6B. Snow-covered fraction exhibits predominantly negative correlations with LST and positive correlations with glacier albedo across most glaciers, with only a small fraction of cases showing opposite behaviour. These relationships are consistent with the expected physical coupling between snow cover, surface energy balance, and reflectivity. Elevation-based relationships are more heterogeneous, with median snow elevation showing moderate consistency but a wider spread of correlation values. This variability likely reflects differences in glacier geometry, hypsometry, and local climatic conditions. Overall, the results indicate that glacier-scale proxies retain physically coherent relationships after deseasonalisation, while revealing meaningful spatial variability in their strength and robustness.

3.6 Dominant glacier-response modes and their structural controls

Principal component analyses (PCA) were applied to trend, variability, and memory metrics derived from glacier-scale proxy time series (Figure 7). In all cases, the first principal component (PC1) captures a large fraction of variance (49.5%, 58.6%, and 73.0% for trend, variability, and memory modes, respectively), indicating coherent response modes across glaciers.

Correlations between PC1 scores and the original glacier proxy metrics provide a physical interpretation of these modes (Figure 8). For the trend mode, positive PC1 scores are associated with conditions consistent with greater snow preservation (higher snow cover and albedo, lower LST), whereas negative scores reflect conditions consistent with glacier degradation. The variability mode captures the amplitude of short-term fluctuations, showing strong positive correlations with variability

https://doi.org/10.5194/egusphere-2026-2386
Preprint. Discussion started: 20 May 2026

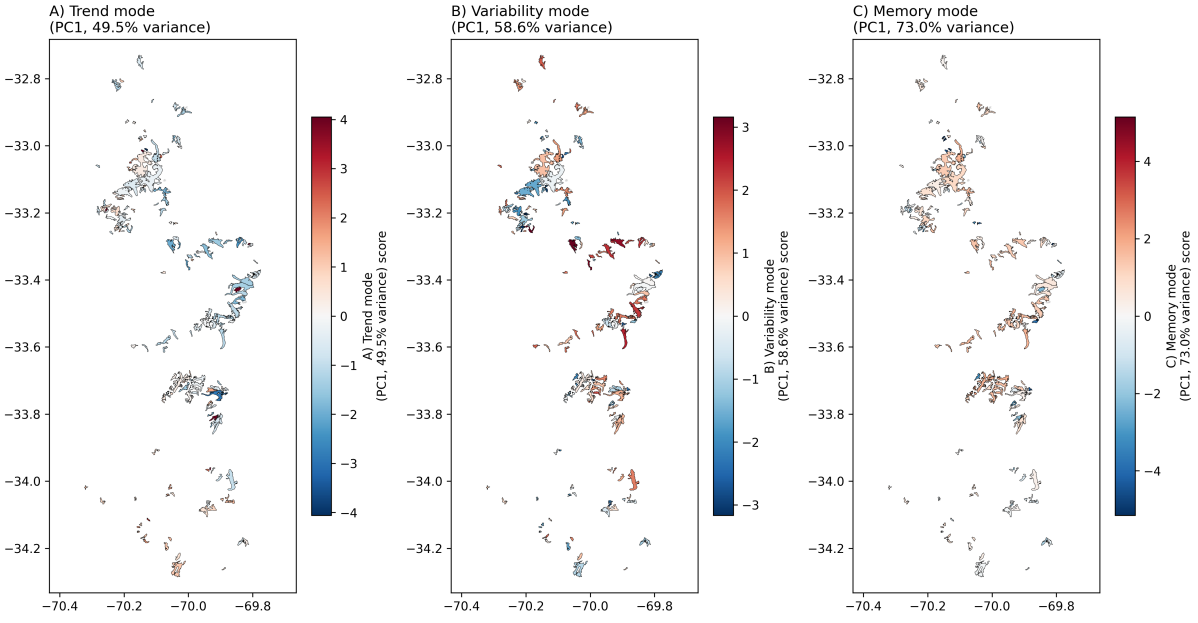

Figure 7. Spatial distribution of dominant glacier-response modes (PC1 scores) for (A) trend, (B) variability, and (C) memory metrics.

metrics across all proxies. The memory mode represents temporal persistence, quantified by lag-1 autocorrelation in glacier proxy time series.

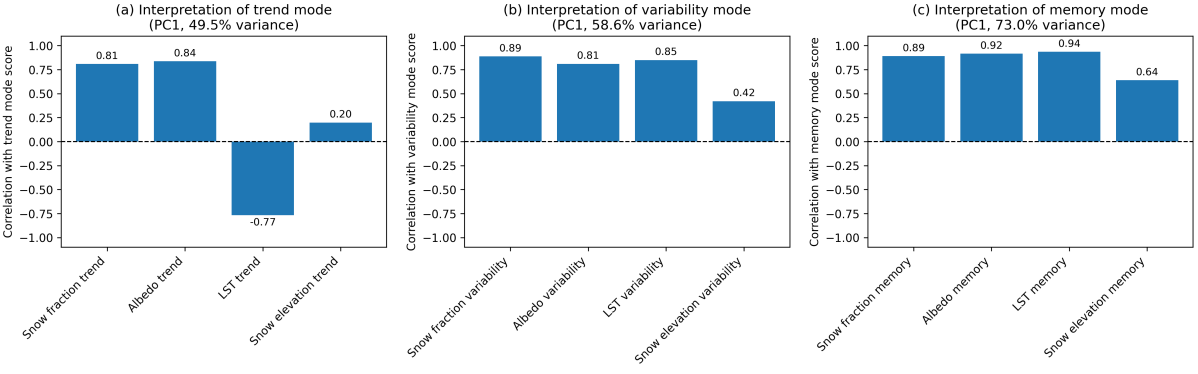

Figure 8. Correlation between PC1 scores and glacier proxy metrics for trend, variability, and memory modes.

Spatial patterns reveal substantial heterogeneity in the expression of these modes (Figure 7). A prevalence of negative trend-mode scores indicates a dominant regional signal of glacier degradation, although local variability in magnitude and direction is evident. Most glaciers exhibit positive memory-mode scores, indicating widespread temporal persistence in glacier dynamics.

https://doi.org/10.5194/egusphere-2026-2386
Preprint. Discussion started: 20 May 2026

To investigate structural controls, PCA scores were correlated with glacier inventory properties (Figure 9). The trend mode shows weak to moderate relationships with glacier characteristics, with the strongest correlation observed for surface slope (r = -0.41), suggesting a dominant climatic control. In contrast, the variability mode is strongly related to elevation (r = -0.52), with lower-elevation glaciers exhibiting greater variability. The memory mode shows the clearest dependence on glacier geometry, with negative correlations with slope (r = -0.46) and elevation (r = -0.40), and positive correlations with thickness and glacier size.

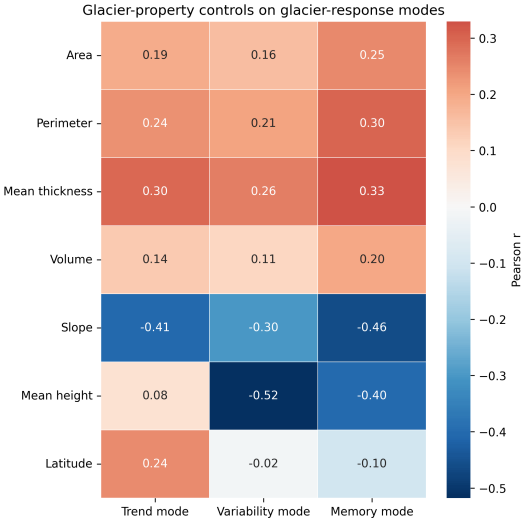

Figure 9. Glacier-property controls on glacier-response modes. The heatmap shows Pearson correlation coefficients between glacier inventory characteristics and the principal component scores representing trend, variability, and memory modes.

Overall, these findings suggest a partial separation between externally forced long-term trends and internally modulated glacier dynamics. While climatic forcing appears to dominate long-term glacier change, glacier geometry contributes to shaping variability and persistence, although these relationships remain moderate. This highlights the combined influence of external forcing and glacier-specific characteristics in driving heterogeneous glacier responses across the study region.

3.7 Lagged response of streamflow and vegetation to glacier proxies

Lagged relationships between glacier snow-covered fraction and streamflow vary systematically across gauging stations, with significant responses observed at both positive and negative lags (Figure 10). Negative lags indicate that glacier variability precedes streamflow, whereas positive lags indicate that streamflow precedes glacier variability.

Negative lags are observed in headwater catchments with stronger glacier influence, suggesting a direct glacier contribution to streamflow. In contrast, some downstream catchments exhibit positive lags, consistent with a progressive decoupling between glacier processes and streamflow along the flow path. However, the spatial distribution of lag responses is heterogeneous,

https://doi.org/10.5194/egusphere-2026-2386
Preprint. Discussion started: 20 May 2026

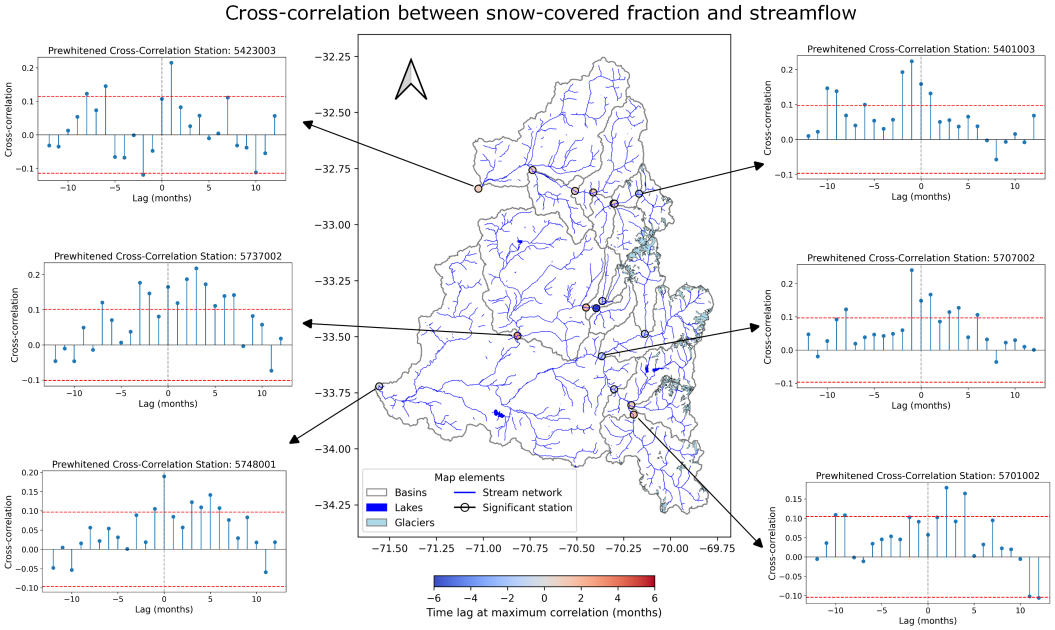

Figure 10. Cross-correlation between glacier snow-covered fraction and streamflow across basins. The central panel shows the spatial distribution of the lag corresponding to the maximum cross-correlation, while surrounding panels illustrate representative prewhitened cross-correlation functions. Red dashed lines in plots indicate approximate significance thresholds.

indicating that these patterns are not uniform across the basin network. Overall, the results suggest a tendency from glacier-influenced responses in headwaters to more integrated hydrological behaviour downstream.

The spatial distribution of vegetation lags also shows a structured pattern (Figure 11). Only a limited number of headwater catchments are retained due to the absence of vegetation, resulting in a dataset restricted to vegetated basins.

Within this subset, negative lags are predominantly observed in intermediate catchments, indicating that glacier variability precedes vegetation activity. Positive lags occur near headwaters and in downstream basins, where vegetation dynamics are less directly coupled to glacier processes.

3.8 Linking glacier-response modes to hydrological lag

To investigate whether glacier-response modes influence downstream hydrological timing, catchment-scale PCA scores were related to the lag of maximum significant cross-correlation between glacier proxies and streamflow using a multiple linear regression model with standardised predictors (Table 2). The model explains a substantial fraction of variability in hydrological lag ($R^2 = 0.72$, $p < 0.01$; Figure 12), indicating strong predictive skill.

The trend mode exhibits a significant positive effect on lag ($\beta = 0.83$, $p = 0.001$), indicating that catchments with more stable glacier conditions (less negative long-term glacier trends) tend to display longer hydrological response times. In contrast,

https://doi.org/10.5194/egusphere-2026-2386
Preprint. Discussion started: 20 May 2026

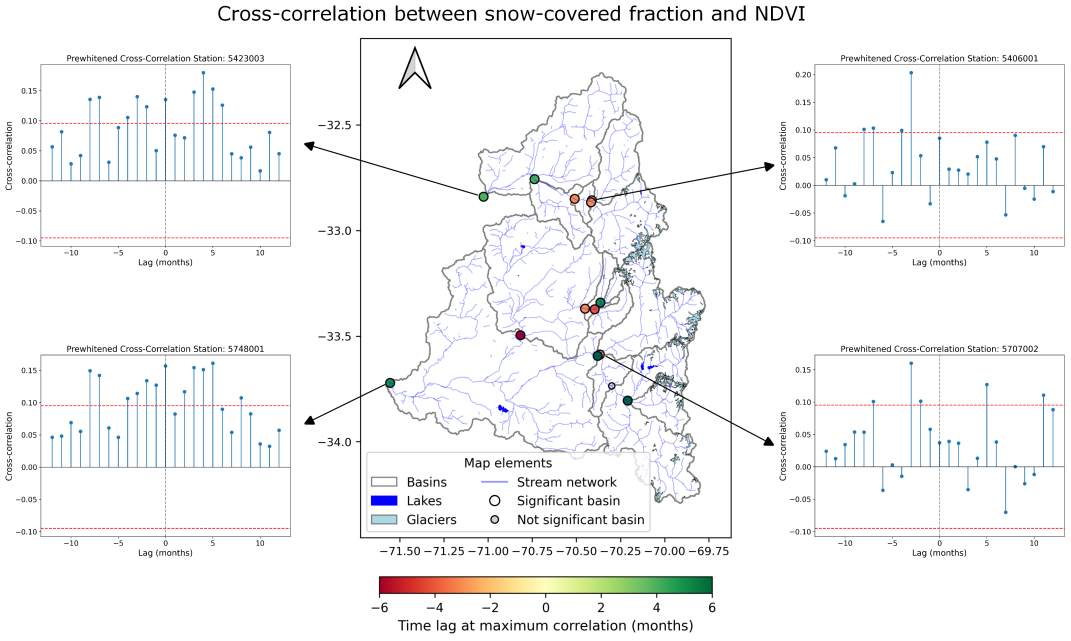

Figure 11. Cross-correlation between glacier snow-covered fraction and NDVI across basins. The central panel shows the spatial distribution of the lag corresponding to the maximum cross-correlation, while surrounding panels illustrate representative prewhitened cross-correlation functions. Red dashed lines in plots indicate approximate significance thresholds.

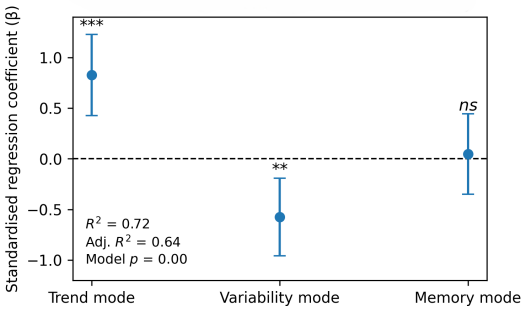

Figure 12. Influence of glacier-response modes on hydrological lag. Standardised regression coefficients ($\beta \pm 95\%$ confidence intervals) from the multiple linear model relating catchment-scale glacier-response modes to the lag of maximum significant cross-correlation with streamflow.

the variability mode shows a significant negative effect ($\beta = -0.57$, $p = 0.007$), indicating faster hydrological responses under higher short-term variability. The memory mode is not statistically significant ($p = 0.80$).

As a sensitivity analysis, the model was re-evaluated using basin-level cluster-robust standard errors to account for potential dependence among nested catchments. Coefficient estimates remained unchanged and the overall interpretation was preserved

https://doi.org/10.5194/egusphere-2026-2386
Preprint. Discussion started: 20 May 2026

Table 2. Multiple linear regression relating glacier-response modes to hydrological lag. Predictors are standardised (z-scores).

Predictor	Coefficient (β)	Std. Error	t-value	p-value	CI (2.5%)	CI (97.5%)
Intercept	0.000	0.161	0.000	1.000	-0.354	0.354
Trend mode	0.826	0.182	4.552	0.001	0.427	1.226
Variability mode	-0.574	0.174	-3.293	0.007	-0.957	-0.190
Memory mode	0.046	0.180	0.257	0.802	-0.351	0.443
Model performance: $R^2 = 0.715$, Adjusted $R^2 = 0.638$, $F = 9.21$, $p = 0.002$.						

(Table S2, Supplementary materials), although the small number of basin groups limits formal inference under clustering. Analogous models fitted for NDVI lag were not statistically significant, suggesting that vegetation response timing is not directly controlled by glacier dynamics.

Overall, these results indicate that hydrological response times emerge from a trade-off between snowpack-mediated storage (captured by the trend mode) and event-scale dynamical variability. While this balance strongly governs streamflow response timing, no statistically significant relationship was found for vegetation response timing, suggesting that NDVI dynamics are not directly controlled by glacier variability within the scope of this analysis.

4 Discussion

The observed glacier-scale changes indicate a coherent regional signal of degradation, characterised by declining snow-covered fraction and albedo, increasing LST, and upward shifts in snow elevation. These patterns are consistent with ongoing glacier retreat under regional warming, as widely documented in the Andes and other mountain systems (Le Quesne et al., 2009; Barcaza et al., 2017; Huss and Hock, 2018). However, the PCA-based decomposition shows that glacier evolution cannot be described by a single trajectory. Instead, glacier behaviour emerges from the interaction between long-term change, short-term variability, and temporal persistence, providing a more nuanced framework for interpreting glacier responses to climatic forcing (Mantelli et al., 2016).

A central finding of this study is that glacier-response modes exert a strong control on the timing of downstream hydrological response. The relationship between PCA-derived modes and streamflow lag indicates that glaciers actively regulate hydrological timing. Catchments characterised by weaker glacier degradation tend to exhibit delayed responses, consistent with the buffering role of snowpack and firn storage (Barnett et al., 2005; Frans et al., 2018). In contrast, systems with higher short-term variability display faster and more direct runoff responses, indicating a shift towards more dynamic, event-driven regimes. This behaviour aligns with previous studies showing that glacier retreat reduces the capacity of mountain systems to store and gradually release water, leading to more variable discharge (Huss and Hock, 2018; Caro et al., 2024). Together, these findings suggest a transition from glacier-mediated buffering towards increased sensitivity to climatic variability.

Vegetation responses exhibit heterogeneous and less systematic behaviour compared to streamflow. Although significant cross-correlations between glacier proxies and NDVI are observed in some catchments, no statistically significant relationship

https://doi.org/10.5194/egusphere-2026-2386
Preprint. Discussion started: 20 May 2026

was found between glacier-response modes and NDVI lag. This indicates that glacier variability does not provide a robust or generalisable explanation of vegetation response timing at the catchment scale. Instead, vegetation dynamics are likely influenced by a broader combination of climatic forcing, soil moisture availability, and land cover characteristics (Forzieri et al., 2017; Zhao et al., 2018). These results suggest that, while glacier signals may contribute to vegetation variability locally, they do not exert a consistent control across catchments in the study region.

Temporal persistence, captured by the memory mode, emerges as a widespread characteristic of glacier dynamics. The strong association with lag-1 autocorrelation indicates that glacier conditions are strongly conditioned by previous states. This behaviour reflects the inherent inertia of glacier systems, where accumulation and melt processes operate over seasonal to multi-annual timescales (Hammond et al., 2018; Marshall, 2021).

The use of satellite-derived proxies highlights the strengths of remote sensing approaches for cryospheric monitoring, enabling the analysis of glacier behaviour across large spatial and temporal scales beyond the limitations of sparse *in situ* observations (Paul et al., 2015; Pellicciotti et al., 2014). In particular, the integration of multiple glacier proxies allows for a physically consistent characterisation of glacier dynamics, capturing long-term trends, short-term variability, and temporal persistence within a unified framework. Uncertainties remain due to the indirect nature of remotely sensed proxies, sensor inconsistencies, and spatial resolution constraints. While vegetation analyses were included as a complementary component, the absence of robust relationships with glacier-response modes suggests that NDVI dynamics are primarily controlled by broader climatic and local factors rather than glacier variability. These results highlight the importance of integrating remote sensing with field-based observations, such as snow water equivalent and glacier volume estimates, to further improve the representation of glacier processes and their hydrological implications.

The implications for water resource management are substantial, particularly in semi-arid regions such as central Chile, where glacier contributions sustain streamflow during dry periods (Vicuña et al., 2011). Glacier retreat not only alters hydrological regimes but also drives cascading impacts on sediment transport, biogeochemical fluxes, and ecosystem functioning (Milner et al., 2017). Additionally, our results indicate that hydrological response times are strongly controlled by the balance between snowpack-mediated storage and short-term variability, suggesting a reduction in natural buffering capacity as glacier systems evolve. This shift towards faster and more variable hydrological responses implies increasing pressure on water supply systems that rely on predictable meltwater contributions.

In practice, water deficits in central Chile are already being mitigated through increased reliance on groundwater extraction, which has become a key adaptive response in recent drought conditions (Alvarez-Garreton et al., 2024; Taucare et al., 2024). However, this strategy may exacerbate long-term sustainability challenges, particularly where recharge is limited. The observed changes in hydrological timing highlight the importance of considering glacier-driven controls on streamflow dynamics in water resource planning. While traditional infrastructure such as reservoirs may partially buffer these changes, their effectiveness ultimately depends on the timing and persistence of inflows, which are influenced by glacier dynamics and snowpack conditions. The observed increase in temporal persistence suggests that streamflow responses may become more conditioned by antecedent states, potentially affecting predictability and management strategies. Alternative adaptation strategies, such as snow retention measures or artificial ice storage, have been proposed in high-mountain environments (Basnet et al., 2015;

https://doi.org/10.5194/egusphere-2026-2386
Preprint. Discussion started: 20 May 2026

Oerlemans et al., 2021), but their applicability remains context-dependent and requires further evaluation under the evolving hydroclimatic conditions identified in this study.

Several limitations should be acknowledged. Nested catchments may introduce dependencies, although sensitivity analyses suggest that the main results are robust. More broadly, advancing the understanding of mountain water systems requires improved integration of observations and models, as well as enhanced high-altitude monitoring (Viviroli et al., 2011). The reliance on proxy-based metrics may not capture subsurface processes such as englacial storage or groundwater interactions (Jansson et al., 2003; Lemieux et al., 2008). In addition, rock glaciers, widespread in the Andes, are difficult to detect using optical remote sensing and may represent important water stores that are not captured in this analysis (Azócar and Brenning, 2010; Jones et al., 2018). Future work should integrate multiple data sources to better constrain glacier-hydrology interactions.

Overall, this study demonstrates that glacier dynamics can be effectively described through complementary modes of change, variability, and persistence, each contributing to the timing of downstream hydrological responses. The results highlight a transition from glacier-buffered to more climate-driven hydrological systems, with important implications for water security in snow- and glacier-dependent regions. By linking glacier behaviour to hydrological response timing and system dynamics, this work provides a framework for understanding how cryospheric change propagates through mountain water systems. While the extension of this framework to ecological responses remains inconclusive at the scales analysed here, it offers a basis for future investigations of coupled hydro-ecological dynamics under changing climatic conditions.

5 Conclusions

This study presents a satellite-based framework to characterise glacier surface dynamics and their lagged influence on downstream hydrological responses, and more limited ecological associations, in central Chile. Multi-decadal Landsat observations reveal a consistent regional signal of glacier degradation, characterised by declining snow cover and albedo, increasing LST, and upward shifts in snow elevation.

The decomposition of glacier behaviour into trend, variability, and memory modes provides a compact and physically meaningful representation of glacier dynamics, highlighting substantial spatial heterogeneity driven by both climatic forcing and glacier-specific characteristics. In particular, variability exhibits strong scale dependence, with contrasting glacier-level and regional trends driven by the disproportionate influence of large glaciers, whereas temporal persistence shows a consistent increase across both glacier and regional scales. Lagged analyses further reveal a transition from glacier-dominated headwater systems, where glacier variability precedes streamflow, to downstream regimes where hydrological responses become increasingly integrated and decoupled from cryospheric processes. Vegetation responses show spatially heterogeneous associations with glacier variability, with some lagged relationships identified through cross-correlation analysis, but no consistent system-scale relationship, as indicated by non-significant regression results.

These findings demonstrate the potential of satellite-derived glacier proxies to quantify the timing and propagation of cryospheric signals in data-scarce regions. Future work should integrate additional observations, including snow water equivalent and glacier thickness estimates, to better constrain water storage and improve predictions under ongoing climate change.

https://doi.org/10.5194/egusphere-2026-2386
Preprint. Discussion started: 20 May 2026

Code availability. The code associated with this project will be made available in the following repository: https://github.com/IFuentesSR/glaciers_assessment

Author contributions. I.F. developed the project. I.F. and S.M. conducted the analysis and research. Results were analyzed by I.F. and S.M. with guidance from I.F. and N.V. The paper was written by I.F. with feedback by N.V. and C.J.

Competing interests. The authors declare they have no conflict of interest.

Acknowledgements. This research was funded by the ANID FONDECYT Iniciacion Project N° 11250007.

During the preparation of this manuscript, the authors used ChatGPT 5.2 for thepurpose of language improvement. The authors have reviewed and edited the output and take fullresponsibility for the content of this publication.

https://doi.org/10.5194/egusphere-2026-2386
Preprint. Discussion started: 20 May 2026

References

Aberle, R., Enderlin, E., O'Neel, S., Florentine, C., Sass, L., Dickson, A., Marshall, H.-P. and Flores, A. (2025), 'Automated snow cover detection on mountain glaciers using spaceborne imagery and machine learning', *The Cryosphere* **19**(4), 1675–1693.

Alvarez-Garreton, C., Boisier, J. P., Garreaud, R., González, J., Rondanelli, R., Gayó, E. and Zambrano-Bigiarini, M. (2024), 'Hess opinions: The unsustainable use of groundwater conceals a "day zero"', *Hydrology and Earth System Sciences* **28**(7), 1605–1616.

Alvarez-Garreton, C., Mendoza, P. A., Boisier, J. P., Addor, N., Galleguillos, M., Zambrano-Bigiarini, M., Lara, A., Puelma, C., Cortes, G., Garreaud, R. et al. (2018), 'The camels-cl dataset: catchment attributes and meteorology for large sample studies–chile dataset', *Hydrology and Earth System Sciences* **22**(11), 5817–5846.

Aprigliano, V., Seriani, S., Toro, C., Rojas, G., Fukushi, M., Cardoso, M., Silva, M. A. V. D., Cucumides, C., de Oliveira, U. R., Henríquez, C. and Braun, A. (2024), 'Built environment effect on metro ridership in metropolitan area of valparaíso, chile, under different influence area approaches', *ISPRS International Journal of Geo-Information* **13**(8), 266.

Ayala, Á., Farías-Barahona, D., Huss, M., Pellicciotti, F., McPhee, J. and Farinotti, D. (2020), 'Glacier runoff variations since 1955 in the maipo river basin, in the semiarid andes of central chile', *The Cryosphere* **14**(6), 2005–2027.

Azócar, G. and Brenning, A. (2010), 'Hydrological and geomorphological significance of rock glaciers in the dry andes, chile (27–33 s)', *Permafrost and Periglacial Processes* **21**(1), 42–53.

Bamber, J. L. and Rivera, A. (2007), 'A review of remote sensing methods for glacier mass balance determination', *Global and Planetary Change* **59**(1-4), 138–148.

Barcaza, G., Nussbaumer, S. U., Tapia, G., Valdés, J., García, J.-L., Videla, Y., Albornoz, A. and Arias, V. (2017), 'Glacier inventory and recent glacier variations in the andes of chile, south america', *Annals of Glaciology* **58**(75pt2), 166–180.

Barnett, T. P., Adam, J. C. and Lettenmaier, D. P. (2005), 'Potential impacts of a warming climate on water availability in snow-dominated regions', *Nature* **438**(7066), 303–309.

Basnet, K., Constantinescu, G., Muste, M. and Ho, H. (2015), 'Method to assess efficiency and improve design of snow fences', *Journal of Engineering Mechanics* **141**(3), 04014136.

Beck, H. E., Zimmermann, N. E., McVicar, T. R., Vergopolan, N., Berg, A. and Wood, E. F. (2018), 'Present and future köppen-geiger climate classification maps at 1-km resolution', *Scientific data* **5**(1), 180214.

Box, G. E., Jenkins, G. M., Reinsel, G. C. and Ljung, G. M. (2015*a*), *Time series analysis: forecasting and control*, John Wiley & Sons.

Box, G. E. P., Jenkins, G. M., Reinsel, G. C. and Ljung, G. M. (2015*b*), *Time Series Analysis: Forecasting and Control*, Wiley Series in Probability and Statistics, 5th edn, John Wiley & Sons, Hoboken, New Jersey.

Bravo, C., Loriaux, T., Rivera, A. and Brock, B. W. (2017), 'Assessing glacier melt contribution to streamflow at universidad glacier, central andes of chile', *Hydrology and Earth System Sciences* **21**(7), 3249–3266.

Caro, A., Condom, T., Rabatel, A., Champollion, N., García, N. and Saavedra, F. (2024), 'Hydrological response of andean catchments to recent glacier mass loss', *The Cryosphere* **18**(5), 2487–2507.

Colin Cameron, A. and Miller, D. L. (2015), 'A practitioner's guide to cluster-robust inference', *Journal of human resources* **50**(2), 317–372.

Crippen, R., Buckley, S., Agram, P., Belz, E., Gurrola, E., Hensley, S., Kobrick, M., Lavalle, M., Martin, J., Neumann, M. et al. (2016), 'Nasadem global elevation model: Methods and progress', *The International Archives of the Photogrammetry, Remote Sensing and Spatial Information Sciences* **41**, 125–128.

https://doi.org/10.5194/egusphere-2026-2386
Preprint. Discussion started: 20 May 2026

Forzieri, G., Alkama, R., Miralles, D. G. and Cescatti, A. (2017), 'Satellites reveal contrasting responses of regional climate to the widespread greening of earth', *Science* **356**(6343), 1180–1184.

Frans, C., Istanbulluoglu, E., Lettenmaier, D. P., Fountain, A. G. and Riedel, J. (2018), 'Glacier recession and the response of summer streamflow in the pacific northwest united states, 1960–2099', *Water Resources Research* **54**(9), 6202–6225.

Fuentes, I., Lopatin, J., Galleguillos, M. and McPhee, J. (2025), 'Vegetation browning as an indicator of drought impact and ecosystem resilience', *Science of Remote Sensing* **11**, 100219.

Garreaud, R. D., Alvarez-Garreton, C., Barichivich, J., Boisier, J. P., Christie, D., Galleguillos, M., LeQuesne, C., McPhee, J. and Zambrano-Bigiarini, M. (2017), 'The 2010–2015 megadrought in central chile: impacts on regional hydroclimate and vegetation', *Hydrology and earth system sciences* **21**(12), 6307–6327.

Garreaud, R. D., Boisier, J. P., Rondanelli, R., Montecinos, A., Sepúlveda, H. H. and Veloso-Aguila, D. (2020), 'The central chile mega drought (2010–2018): a climate dynamics perspective', *International Journal of Climatology* **40**(1), 421–439.

Gascoin, S., Kinnard, C., Ponce, R., Lhermitte, S., MacDonell, S. and Rabatel, A. (2011), 'Glacier contribution to streamflow in two head-waters of the huasco river, dry andes of chile', *The Cryosphere* **5**(4), 1099–1113.

Gorelick, N., Hancher, M., Dixon, M., Ilyushchenko, S., Thau, D. and Moore, R. (2017), 'Google earth engine: Planetary-scale geospatial analysis for everyone', *Remote sensing of Environment* **202**, 18–27.

Greuell, W. and Knap, W. H. (2000), 'Remote sensing of the albedo and detection of the slush line on the greenland ice sheet', *Journal of Geophysical Research: Atmospheres* **105**(D12), 15567–15576.

Gunnarsson, A., Gardarsson, S. M. and Pálsson, F. (2023), 'Modeling of surface energy balance for icelandic glaciers using remote-sensing albedo', *The Cryosphere* **17**(9), 3955–3986.

Hammond, J. C., Saavedra, F. A. and Kampf, S. K. (2018), 'Global snow zone maps and trends in snow persistence 2001–2016', *International Journal of Climatology* **38**(12), 4369–4383.

Hanzer, F., Förster, K., Nemec, J. and Strasser, U. (2018), 'Projected cryospheric and hydrological impacts of 21st century climate change in the ötztal alps (austria) simulated using a physically based approach', *Hydrology and Earth System Sciences* **22**(2), 1593–1614.

Hijmans, R. J., Cameron, S. E., Parra, J. L., Jones, P. G. and Jarvis, A. (2005), 'Very high resolution interpolated climate surfaces for global land areas', *International Journal of Climatology: A Journal of the Royal Meteorological Society* **25**(15), 1965–1978.

Hock, R. (2005), 'Glacier melt: a review of processes and their modelling', *Progress in physical geography* **29**(3), 362–391.

Huss, M., Bookhagen, B., Huggel, C., Jacobsen, D., Bradley, R. S., Clague, J. J., Vuille, M., Buytaert, W., Cayan, D. R., Greenwood, G. et al. (2017), 'Toward mountains without permanent snow and ice', *Earth's Future* **5**(5), 418–435.

Huss, M. and Hock, R. (2018), 'Global-scale hydrological response to future glacier mass loss', *Nature Climate Change* **8**(2), 135–140.

Irons, J. R., Dwyer, J. L. and Barsi, J. A. (2012), 'The next landsat satellite: The landsat data continuity mission', *Remote sensing of environment* **122**, 11–21.

Jansson, P., Hock, R. and Schneider, T. (2003), 'The concept of glacier storage: a review', *Journal of Hydrology* **282**(1-4), 116–129.

Jiao, Y., Lei, H., Yang, D., Huang, M., Liu, D. and Yuan, X. (2017), 'Impact of vegetation dynamics on hydrological processes in a semi-arid basin by using a land surface-hydrology coupled model', *Journal of Hydrology* **551**, 116–131.

Jolliffe, I. T. and Cadima, J. (2016), 'Principal component analysis: a review and recent developments', *Philosophical transactions of the royal society A: Mathematical, Physical and Engineering Sciences* **374**(2065), 20150202.

Jones, D., Harrison, S., Anderson, K. and Betts, R. (2018), 'Mountain rock glaciers contain globally significant water stores', *Scientific Reports* **8**(1), 2834.

https://doi.org/10.5194/egusphere-2026-2386
Preprint. Discussion started: 20 May 2026

Jpl, N. (2020), 'Nasadem merged dem global 1 arc second v001', *NASA EOSDIS Land Processes Distributed Active Archive Center (DAAC) data set* pp. NASADEM_HGT–001.

Le Quesne, C., Acuña, C., Boninsegna, J. A., Rivera, A. and Barichivich, J. (2009), 'Long-term glacier variations in the central andes of argentina and chile, inferred from historical records and tree-ring reconstructed precipitation', *Palaeogeography, Palaeoclimatology, Palaeoecology* **281**(3-4), 334–344.

Lemieux, J.-M., Sudicky, E. A., Peltier, W. R. and Tarasov, L. (2008), 'Simulating the impact of glaciations on continental groundwater flow systems: 1. relevant processes and model formulation', *Journal of Geophysical Research: Earth Surface* **113**(F3).

Li, M., Cao, S., Zhu, Z., Wang, Z., Myneni, R. B. and Piao, S. (2023), 'Spatiotemporally consistent global dataset of the gimms normalized difference vegetation index (pku gimms ndvi) from 1982 to 2022', *Earth System Science Data* **15**(9), 4181–4203.

Liang, S. (2001), 'Narrowband to broadband conversions of land surface albedo i: Algorithms', *Remote sensing of environment* **76**(2), 213–238.

Liu, M., Adam, J. C., Richey, A. S., Zhu, Z. and Myneni, R. B. (2018), 'Factors controlling changes in evapotranspiration, runoff, and soil moisture over the conterminous us: Accounting for vegetation dynamics', *Journal of Hydrology* **565**, 123–137.

Mantelli, E., Bertagni, M. B. and Ridolfi, L. (2016), 'Stochastic ice stream dynamics', *Proceedings of the National Academy of Sciences* **113**(32), E4594–E4600.

Markham, B. L. and Helder, D. L. (2012), 'Forty-year calibrated record of earth-reflected radiance from landsat: A review', *Remote Sensing of Environment* **122**, 30–40.

Marshall, S. J. (2021), 'Regime shifts in glacier and ice sheet response to climate change: examples from the northern hemisphere', *Frontiers in Climate* **3**, 702585.

Masek, J. G., Wulder, M. A., Markham, B., McCorkel, J., Crawford, C. J., Storey, J. and Jenstrom, D. T. (2020), 'Landsat 9: Empowering open science and applications through continuity', *Remote Sensing of Environment* **248**, 111968.

Masiokas, M. H., Christie, D. A., Le Quesne, C., Pitte, P., Ruiz, L., Villalba, R., Luckman, B. H., Berthier, E., Nussbaumer, S. U., González-Reyes, Á. et al. (2016), 'Reconstructing the annual mass balance of the echaurren norte glacier (central andes, 33.5° s) using local and regional hydroclimatic data', *The Cryosphere* **10**(2), 927–940.

Menenti, M., Li, J., Mancini, M., Li, X., Pellicciotti, F., Yang, K. et al. (2020), 'High elevation energy and water balance: the roles of surface albedo and temperature', *Journal of Geodesy and Geoinformation Science* **3**(4), 70.

Mernild, S. H., Liston, G. E., Hiemstra, C., Beckerman, A. P., Yde, J. C. and McPhee, J. (2017), 'The andes cordillera. part iv: spatio-temporal freshwater run-off distribution to adjacent seas (1979–2014)', *International Journal of Climatology* **37**(7), 3175–3196.

Milner, A. M., Khamis, K., Battin, T. J., Brittain, J. E., Barrand, N. E., Füreder, L., Cauvy-Fraunié, S., Gíslason, G. M., Jacobsen, D., Hannah, D. M. et al. (2017), 'Glacier shrinkage driving global changes in downstream systems', *Proceedings of the National Academy of Sciences* **114**(37), 9770–9778.

Miranda, A., Syphard, A. D., Berdugo, M., Carrasco, J., Gómez-González, S., Ovalle, J. F., others and Garreaud, R. (2023), 'Widespread synchronous decline of mediterranean-type forest driven by accelerated aridity', *Nature Plants* **9**(11), 1810–1817.

Nie, Y., Pritchard, H. D., Liu, Q., Hennig, T., Wang, W., Wang, X., Liu, S., Nepal, S., Samyn, D., Hewitt, K. et al. (2021), 'Glacial change and hydrological implications in the himalaya and karakoram', *Nature reviews earth & environment* **2**(2), 91–106.

Oerlemans, J. (2005), 'Extracting a climate signal from 169 glacier records', *science* **308**(5722), 675–677.

Oerlemans, J., Balasubramanian, S., Clavuot, C. and Keller, F. (2021), 'Brief communication: Growth and decay of an ice stupa in alpine conditions–a simple model driven by energy-flux observations over a glacier surface', *The Cryosphere* **15**(6), 3007–3012.

https://doi.org/10.5194/egusphere-2026-2386
Preprint. Discussion started: 20 May 2026

Ohlanders, N., Rodriguez, M. and McPhee, J. (2013), 'Stable water isotope variation in a central andean watershed dominated by glacier and snowmelt', *Hydrology and Earth System Sciences* **17**(3), 1035–1050.

Owen, L. A., Thackray, G., Anderson, R. S., Briner, J., Kaufman, D., Roe, G., Pfeffer, W. and Yi, C. (2009), 'Integrated research on mountain glaciers: current status, priorities and future prospects', *Geomorphology* **103**(2), 158–171.

Paul, F., Bolch, T., Kääb, A., Nagler, T., Nuth, C., Scharrer, K., Shepherd, A., Strozzi, T., Ticconi, F., Bhambri, R. et al. (2015), 'The glaciers climate change initiative: Methods for creating glacier area, elevation change and velocity products', *Remote Sensing of Environment* **162**, 408–426.

Pellicciotti, F., Ragettli, S., Carenzo, M. and McPhee, J. (2014), 'Changes of glaciers in the andes of chile and priorities for future work', *Science of the Total Environment* **493**, 1197–1210.

Pettorelli, N., Vik, J. O., Mysterud, A., Gaillard, J.-M., Tucker, C. J. and Stenseth, N. C. (2005), 'Using the satellite-derived ndvi to assess ecological responses to environmental change', *Trends in ecology & evolution* **20**(9), 503–510.

Politis, D. N. and Romano, J. P. (1994), 'The stationary bootstrap', *Journal of the American Statistical association* **89**(428), 1303–1313.

Pradhananga, D. and Pomeroy, J. W. (2022), 'Recent hydrological response of glaciers in the canadian rockies to changing climate and glacier configuration', *Hydrology and Earth System Sciences* **26**(10), 2605–2616.

Rabatel, A., Francou, B., Soruco, A., Gomez, J., Cáceres, B., Ceballos, J. L., Basantes, R., Vuille, M., Sicart, J.-E., Huggel, C. et al. (2013), 'Current state of glaciers in the tropical andes: a multi-century perspective on glacier evolution and climate change', *The Cryosphere* **7**(1), 81–102.

Rabatel, A., Sirguey, P., Drolon, V., Maisongrande, P., Arnaud, Y., Berthier, E., Davaze, L., Dedieu, J.-P. and Dumont, M. (2017), 'Annual and seasonal glacier-wide surface mass balance quantified from changes in glacier surface state: A review on existing methods using optical satellite imagery', *Remote Sensing* **9**(5), 507.

Racoviteanu, A. E., Nicholson, L. and Glasser, N. F. (2021), 'Surface composition of debris-covered glaciers across the himalaya using linear spectral unmixing of landsat 8 oli imagery', *The Cryosphere* **15**(9), 4557–4588.

Racoviteanu, A. E., Paul, F., Raup, B., Khalsa, S. J. S. and Armstrong, R. (2009), 'Challenges and recommendations in mapping of glacier parameters from space: results of the 2008 global land ice measurements from space (glims) workshop, boulder, colorado, usa', *Annals of Glaciology* **50**(53), 53–69.

Racoviteanu, A. E., Williams, M. W. and Barry, R. G. (2008), 'Optical remote sensing of glacier characteristics: a review with focus on the himalaya', *Sensors* **8**(5), 3355–3383.

Radić, V. and Hock, R. (2014), 'Glaciers in the earth's hydrological cycle: assessments of glacier mass and runoff changes on global and regional scales', *Surveys in Geophysics* **35**(3), 813–837.

Rastner, P., Prinz, R., Notarnicola, C., Nicholson, L., Sailer, R., Schwaizer, G. and Paul, F. (2019), 'On the automated mapping of snow cover on glaciers and calculation of snow line altitudes from multi-temporal landsat data', *Remote Sensing* **11**(12), 1410.

Raup, B., Kääb, A., Kargel, J. S., Bishop, M. P., Hamilton, G., Lee, E., Paul, F., Rau, F., Soltesz, D., Khalsa, S. J. S. et al. (2007), 'Remote sensing and gis technology in the global land ice measurements from space (glims) project', *Computers & geosciences* **33**(1), 104–125.

Rodriguez, M., Ohlanders, N. and McPhee, J. (2014), 'Estimating glacier and snowmelt contributions to stream flow in a central andes catchment in chile using natural tracers', *Hydrology and Earth System Sciences Discussions* **11**(7), 8949–8994.

Roy, D. P., Wulder, M. A., Loveland, T. R., Ce, W., Allen, R. G., Anderson, M. C., Helder, D., Irons, J. R., Johnson, D. M., Kennedy, R. et al. (2014), 'Landsat-8: Science and product vision for terrestrial global change research', *Remote sensing of Environment* **145**, 154–172.

https://doi.org/10.5194/egusphere-2026-2386
Preprint. Discussion started: 20 May 2026

Salomonson, V. V. and Appel, I. (2004), 'Estimating fractional snow cover from modis using the normalized difference snow index', *Remote sensing of environment* **89**(3), 351–360.

Salomonson, V. V. and Appel, I. (2006), 'Development of the aqua modis ndsi fractional snow cover algorithm and validation results', *IEEE Transactions on Geoscience and Remote Sensing* **44**(7), 1747–1756.

Shumway, R. H. and Stoffer, D. S. (2017), Arima models, *in* 'Time series analysis and its applications: with R examples', Springer, pp. 75–163.

Smith, J. A., Lin, T. and Ranson, K. J. (1980), 'The lambertian assumption and landsat data', *Photogrammetric Engineering and Remote Sensing* **46**(9), 1183–1189.

Sobrino, J. A., Jiménez-Muñoz, J. C. and Paolini, L. (2004), 'Land surface temperature retrieval from landsat tm 5', *Remote Sensing of environment* **90**(4), 434–440.

Stewart, I. T. (2009), 'Changes in snowpack and snowmelt runoff for key mountain regions', *Hydrological Processes: An International Journal* **23**(1), 78–94.

Taucare, M., Viguier, B., Figueroa, R. and Daniele, L. (2024), 'The alarming state of central chile's groundwater resources: A paradigmatic case of a lasting overexploitation', *Science of The Total Environment* **906**, 167723.

Teillet, P. M., Guindon, B. and Goodenough, D. G. (1982), 'On the slope-aspect correction of multispectral scanner data', *Canadian Journal of Remote Sensing* **8**(2), 84–106.

Traversa, G., Fugazza, D., Senese, A. and Frezzotti, M. (2021), 'Landsat 8 oli broadband albedo validation in antarctica and greenland', *Remote Sensing* **13**(4), 799.

Vicuña, S., Garreaud, R. D. and McPhee, J. (2011), 'Climate change impacts on the hydrology of a snowmelt driven basin in semiarid chile', *Climatic Change* **105**(3), 469–488.

Viviroli, D., Archer, D. R., Buytaert, W., Fowler, H. J., Greenwood, G. B., Hamlet, A. F., Huang, Y., Koboltschnig, G., Litaor, M., López-Moreno, J. I. et al. (2011), 'Climate change and mountain water resources: overview and recommendations for research, management and policy', *Hydrology and Earth System Sciences* **15**(2), 471–504.

Webb, M. J., Winter, J. M., Spera, S. A., Chipman, J. W. and Osterberg, E. C. (2021), 'Water, agriculture, and climate dynamics in central chile's aconcagua river basin', *Physical Geography* **42**(5), 395–415.

Winkler, S., Chinn, T., Gärtner-Roer, I., Nussbaumer, S. U., Zemp, M. and Zumbühl, H. J. (2010), 'An introduction to mountain glaciers as climate indicators with spatial and temporal diversity', *Erdkunde* pp. 97–118.

Wu, P., Shen, H., Zhang, L. and Göttsche, F.-M. (2015), 'Integrated fusion of multi-scale polar-orbiting and geostationary satellite observations for the mapping of high spatial and temporal resolution land surface temperature', *Remote Sensing of Environment* **156**, 169–181.

Yin, D., Cao, X., Chen, X., Shao, Y. and Chen, J. (2013), 'Comparison of automatic thresholding methods for snow-cover mapping using landsat tm imagery', *International Journal of Remote Sensing* **34**(19), 6529–6538.

Zemp, M., Frey, H., Gärtner-Roer, I., Nussbaumer, S. U., Hoelzle, M., Paul, F., Haeberli, W., Denzinger, F., Ahlstrøm, A. P., Anderson, B. et al. (2015), 'Historically unprecedented global glacier decline in the early 21st century', *Journal of glaciology* **61**(228), 745–762.

Zemp, M., Huss, M., Thibert, E., Eckert, N., McNabb, R., Huber, J., Barandun, M., Machguth, H., Nussbaumer, S. U., Gärtner-Roer, I. et al. (2019), 'Global glacier mass changes and their contributions to sea-level rise from 1961 to 2016', *Nature* **568**(7752), 382–386.

Zhao, L., Dai, A. and Dong, B. (2018), 'Changes in global vegetation activity and its driving factors during 1982–2013', *Agricultural and Forest Meteorology* **249**, 198–209.

https://doi.org/10.5194/egusphere-2026-2386
Preprint. Discussion started: 20 May 2026

Zwiers, F. W. and Von Storch, H. (2004), 'On the role of statistics in climate research', *International Journal of Climatology: A Journal of the Royal Meteorological Society* **24**(6), 665–680.